Received 18 November 2022, accepted 30 November 2022, date of publication 16 December 2022,
date of current version 21 December 2022.

Digital Object Identifier 10.1109/ACCESS.2022.3227859

RESEARCH ARTICLE

Optimal Operation of Compressors in an Integrated Gas and Electricity System–An Enhanced MISOCP Method

QIKUN CHEN[1], YONGNING ZHAO[2], MEYSAM QADRDAN[1], (Senior Member, IEEE), AND NICHOLAS JENKINS[1], (Fellow, IEEE)
[1]School of Engineering, Cardiff University, CF24 3AA Cardiff, U.K.
[2]College of Information and Electric Engineering, China Agricultural University, Beijing 100107, China

Corresponding author: Meysam Qadrdan (qadrdanm@cardiff.ac.uk)

This work was supported in part by the U.K. Engineering and Physical Sciences Research Council (EPSRC) through project titled MaxImiSing Flexibility Through Multi-Scale IntegratiON of Energy Systems (MISSION) under Grant EP/S001492/1, and in part by the Chinese Scholarship Council provided Ph.D. studentship to Qikun Chen under Grant 202009225006.

ABSTRACT The optimal operation of gas-driven compressors (GDCs) and electric-driven compressors (EDCs) was investigated to minimise the cost of operating a gas network. The operational optimisation model of the gas network with relatively detailed representation of gas compressors was formulated as a Mixed-Integer Second Order Cone Programming (MISOCP) problem. A bound-tightening algorithm was used to improve the quality of the solution from the relaxed MISOCP formulation. Using this model, the operation of the high-pressure gas transmission network in South Wales and Southwest of England was optimised considering day-ahead gas and electricity prices. The results show that, compared to the case in which only gas-driven compressors are available, nearly 63% of the operating cost of the gas network can be reduced through coordinated operation of gas-driven and electric-driven compressors, while it produces only 36% of carbon dioxide emissions compared of case that only gas-driven compressors are allowed to work. Although, these specific figures for cost and emission reductions depend on electricity and gas prices, as well as emission intensity of the power grid, the results demonstrate the potential for using the inherent flexibility of the high pressure gas network to reduce its operating cost and emission, and to support the operation of power systems. The within-pipe storage capability (i.e., linepack) of the high-pressure gas network is a key enabler that allows electric-driven compressors to shift their operation schedule in time to benefit from low electricity prices.

INDEX TERMS Bound-tightening algorithm, electric-driven gas compressors, integrated electricity and gas network, MISOCP, optimal operation.

NOMENCLATURE

A. SETS

I	set of gas network nodes i
GT	set of gas terminals gt (GT $\subset I$)
A	set of pipelines (i, j)
C	set of compressors c ($C \subset A$)
D	set of gas demand nodes d ($D \subset I$)
E	subset of electric-driven compressors e ($E \subset C$)
G	subset of gas-driven compressors g ($G \subset C$)
T	set of timesteps t
AS_i	set of assets located at node i

B. VARIABLES

$P_{c,t}$	energy consumption of a compressor c in time step t (MWh)
$P_{e,t}$	energy consumption of an electric-driven compressor e in time step t (MWh)
$P_{g,t}$	energy consumption of a gas driven compressor g in time step t (MWh)

The associate editor coordinating the review of this manuscript and approving it for publication was Mostafa M. Fouda.

$p_{i,t}$ nodal pressure at node i in time step t (bar)
$f_{\mathrm{gt},t}$ gas supply from terminal gt in time step t ($\mathrm{Mm^3/h}$)
$f_{d,t}$ gas demand at node d in time step t ($\mathrm{Mm^3/h}$)
$f_{i,j,t}$ average value of gas flow in pipeline (i,j) in time step t ($\mathrm{Mm^3/h}$)
$f_{i,j,t}^{\mathrm{in/out}}$ inflow/outflow of gas in pipeline (i,j) in time step t ($\mathrm{Mm^3/h}$)
$f_{i,j,t}^{+/-}$ gas flows through pipeline (i,j) from i to j (positive direction)/from j to i(negative direction) ($\mathrm{Mm^3/h}$)
$L_{i,j,t}$ linepack in pipeline (i,j) in time step t ($\mathrm{Mm^3}$)
$\alpha_{c,t}$ compression ratio of compressor c in time step t.
$Q_{c,t}$ gas throughput of compressor c in time step t ($\mathrm{Mm^3/h}$)
$Q'_{g,t}$ gas consumed by a gas-driven compressor g in time step t ($\mathrm{Mm^3/h}$)

C. PARAMETERS

C_t^{G} gas price in time step t (GBP/ $\mathrm{Mm^3}$)
C_t^{E} electricity price in time step t (GBP/MWh)
Ø energy content of natural gas in standard temperature and pressure condition (10.55 MWh/ $\mathrm{km^3}$)
$p_{i,t}^{\min}$ minimum pressure of node i in time step t (bar)
$p_{i,t}^{\max}$ maximum pressure of node i in time step t (bar)
$f_{gt,t}^{\min}$ minimum gas supply of gas terminal gt in time step t ($\mathrm{Mm^3/h}$)
$f_{gt,t}^{\max}$ maximum gas supply of gas terminal gt in time step t ($\mathrm{Mm^3/h}$)
$f_{i,j,t}^{\min}$ minimum gas flow of pipeline (i,j) in time step t ($\mathrm{Mm^3/h}$)
$f_{i,j,t}^{\max}$ maximum gas flow of pipeline (i,j) in time step t ($\mathrm{Mm^3/h}$)
$L_{i,j}^0$ initial linepack in pipeline (i,j) (linepack at time 0) ($\mathrm{Mm^3}$)
$S_{i,j}$ linepack coefficient in pipeline (i,j) ($\mathrm{Mm^3/bar}$)
$K_{i,j}$ gas flow coefficient in pipeline (i,j) ($\mathrm{Mm^3/h/bar}$)
R diameter of a pipe (mm)
Z compressibility of gas
T_{b} base temperature of gas flow (K)
L length of a pipe (km)
r density of gas (kg/ $\mathrm{m^3}$)
B, B' fitted coefficients of a linear expression used for simplifying the nonlinear equation of compressors energy consumption
m polytropic exponent of a compressor unit ($m = 1.3$)
η efficiency of a compressor unit ($\eta = 0.8$)
$\bar{f}_{i,j,t}^{+/-}$ maximum value of positive/negative gas flow of pipeline (i,j) in time step t ($\mathrm{Mm^3/h}$)
$\underline{f}_{i,j,t}^{+/-}$ minimum value of positive/negative gas flow of pipeline (i,j) in time step t ($\mathrm{Mm^3/h}$)
$\underline{\pi}_{i,j,t}^{+/-}$ minimum value of $pr_{i,t}+pr_{j,t}/pr_{i,t}-pr_{j,t}$ in time step t (bar)
$\bar{\pi}_{i,j,t}^{+/-}$ maximum value of $pr_{i,t}+pr_{j,t}/pr_{i,t}-pr_{j,t}$ in time step t (bar)
γ_k parameter for tightening bound
δ defined convergence tolerance
N_{it} number of iterations

I. INTRODUCTION

A. BACKGROUND

The gas network plays an important role in the Great Britain (GB) in supplying gas for heating and electricity generation. Gas presently satisfies 85% of residential heat demand and almost 40% of electricity is generated by gas-fired power plants [1]. Although, gas demand in the future is expected to decrease to meet the decarbonisation target, the gas network has the potential to support the operation of low carbon electricity systems through providing flexibility to compensate for variable renewable generation, as the gas-fired power plants can be rapidly and flexibly dispatched by making use of linepack and gas storage [2], [3], [4], [5].

Compressor units are of great importance in directing flows, boosting the gas pressure, and maintaining the level of linepack. The national transmission system (NTS) in the GB has 24 compressor sites with 75 compressor units [1]. Mainly, gas-driven compressor (GDC) units are employed which results in the emission of various gases [6]. Under the Industrial Emission Directive (IED) [6], the network operator is required to reduce emissions from the compressor fleet. One option is to replace gas-driven compressors with electric-driven compressors (EDCs). As of 2018, there were 9 electric-driven compressor units installed in the NTS with total power capacity of nearly 200 MW [7].

A combination of the GDCs and the EDCs can provide flexibility to the power system by shifting electricity consumption of electric-driven compressors in time (using linepack as buffer) and switching between gas and electricity to fuel compressors. The GDC units will be used when the gas price is lower than that of electricity, and the electric-driven compressor (EDC) will be used when the electricity price is lower, or the compressors can be scheduled to reduce the emission from compressor fleet, i.e., using electric-driven compressors when the emission intensity of the electricity grid is lower than the emission intensity of natural gas.

Although, the optimal operation of gas networks has been widely analysed, most of the literatures neglected flexibility that can be provided by the use of compressor units. To exploit the potential flexibility of the compressors alongside the linepack, it is necessary to model the compressor units in the model of the gas network.

B. LITERATURE REVIEW

Flexibility of the integrated gas and electricity system has been widely investigated though there has been limited research focused on clarifying the role of compressor units. To reduce complexity, the model of the compressor units was simplified to an abstract compressing ratio in most research as [8], [9], and [10]. However, only taking account of the compressing ratio in the modelling of the compressors cannot reveal the benefit of the compressor unit e.g., providing flexibility to operate the gas network and gas-fired power plant [7].

There is a relatively large number of literature that studied the detailed behaviour of gas compressor units. In [11], the authors improved the accuracy of simulating the operational envelope of a gas compressor by considering the compressibility and energy loss of gas flow within the compressor. Reference [12] analysed the efficiency and fuel consumption of a compressor, under different thermal environments. Literature [13] modelled the compressor units in both serial and parallel, and used the load-sharing optimisation (LSO) to find the optimal operation with minimum cost of the compressor units. These research are looking for a better performance of the compressor unit in operation under various conditions (varying demand load, temperature changes, etc), and hence to reduce the cost via optimal operation of the compressor units. They are significant in clarifying the function of compressors in boosting the pressure to meet the operational requirements, however, the interactions between the operation of the compressors and the wider gas networks that are necessary for quantifying magnitude and value of flexibility from compressors were not considered. Taking into account the compressor units into the problem of gas networks operational optimisation greatly increase the computational complexity, as the power consumption of gas compressors and their operating envelops is nonlinear and nonconvex. Hence, a reasonable simplification and effective solution algorithm are essential in numerical modelling.

When exploring the optimal operation of gas networks, the steady state gas flow equation, which is nonlinear and nonconvex, brings a significant challenge. Using the nonlinear gas flow equation [14], [15], [16], [17] increases computation time while simplifying it to a linear expression [18] may not accurately describe the relationship between gas flow and pressure drop. Piece-wise linearisation (PWL), which replaces the nonlinear term with several linear segments, shows good performance in the approximation of the gas flow equation and has been widely used [19], [20], [21], [22], [23]. Compared with PWL, Second Order Cone Programming (SOCP) is generally faster, e.g., a 100 times faster computation speed is obtained in a case study [24] by using the SOCP approximation in comparison with using PWL. However, this approach is less accurate if the bounds of SOC constraints are not tight enough. To address this, enhanced SOCP with a bound-tightening algorithm proposed in reference [8] can be helpful. By using this method, the bound of SOC constraints which are over relaxed can be gradually tightened until reaching the satisfying tolerance. This algorithm was used and extended in this paper to solve the optimisation problem of gas network operation considering the flexible operation of gas compressors.

The main contributions of this paper are: (a) formulating the operation of a high pressure gas network, considering detailed representation of gas-driven and electric-driven compressor units, as an MISOCP, (b) improving the accuracy of the optimum solution using a bound-tightening method, and (c) quantifying the magnitude and value of flexibility from coordinated operation of gas-driven and electric-driven compressors.

II. MODELING OF THE GAS NETWORK

A. PROBLEM FORMULATION

The operational optimisation of the gas network was formulated to minimise its operating cost over 24 hours, subject to physical and operating constraints of the components as (2) - (15). The objective function of the optimisation problem was shown in (1), where the $C_t^{\mathrm{G}} f_{gt,t}$, is the cost of gas supply (gas consumed by compressor units was included), and $C_t^{\mathrm{E}} P_{e,t}$ is the cost of electricity consumed by electric-driven compressors.

$$\mathrm{Min}\ \sum_{t=1}^{24} \left(\sum_{\mathrm{gt}\in\mathrm{GT}} C_t^{\mathrm{G}} f_{\mathrm{gt},t} + \sum_{e\in E} C_t^{\mathrm{E}} P_{e,t}\right) \tag{1}$$

$$p_i^{\min} \le p_{i,t} \le p_i^{\max}, \quad \forall i, t, \tag{2}$$

$$f_{i,j,t}^{\min} \le f_{i,j,t} \le f_{i,j,t}^{\max}, \quad \forall (i,j) \in A, t, \tag{3}$$

$$f_{\mathrm{gt},t}^{\min} \le f_{\mathrm{gt},t} \le f_{\mathrm{gt},t}^{\max}, \quad \forall \mathrm{gt}, t, \tag{4}$$

$$\sum_{\mathrm{gt}\in\mathrm{AS}_{\mathrm{i}}^{\mathrm{gt}}} f_{\mathrm{gt},t} - \sum_{i:(j,i)\in A} \left(f_{i,j,t}^{\mathrm{in}} - f_{j,i,t}^{\mathrm{out}}\right) = \sum_{d\in\mathrm{AS}_{\mathrm{i}}^{d}} f_{d,t}, \quad \forall i, t, \tag{5}$$

$$f_{i,j,t}\left|f_{i,j,t}\right| = K_{i,j}^2 \left(p_{i,t}^2 - p_{j,t}^2\right), \quad \forall (i,j) \in A, t, \tag{6}$$

$$f_{i,j,t}^{+} = \frac{f_{i,j,t}^{\mathrm{in}} + f_{i,j,t}^{\mathrm{out}}}{2}, \quad \forall (i,j) \in A, t, \tag{7}$$

$$f_{i,j,t}^{-} = \frac{f_{j,i,t}^{\mathrm{in}} + f_{j,i,t}^{\mathrm{out}}}{2}, \quad \forall (i,j) \in A, t, \tag{8}$$

$$0 \le f_{i,j,t}^{+} \le M x_{i,j,t}, \quad \forall (i,j) \in A, t, \tag{9}$$

$$0 \le f_{i,j,t}^{-} \le M(1 - x_{i,j,t}), \quad \forall (i,j) \in A, t, \tag{10}$$

$$f_{i,j,t} = f_{i,j,t}^{+} - f_{i,j,t}^{-}, \quad \forall (i,j) \in A, t, \tag{11}$$

$$L_{i,j,t} = S_{i,j} \frac{(p_{i,t} + p_{j,t})}{2}, \quad \forall (i,j) \in A, t, \tag{12}$$

$$L_{i,j,t} = L_{i,j}^0 + f_{i,j,t}^{\mathrm{in}} - f_{i,j,t}^{\mathrm{out}} + f_{j,i,t}^{\mathrm{in}} - f_{j,i,t}^{\mathrm{out}}, \quad \forall (i,j) \in A, t = 1, \tag{13}$$

$$L_{i,j,t} = L_{i,j,t-1} + f_{i,j,t}^{\mathrm{in}} - f_{i,j,t}^{\mathrm{out}} + f_{j,i,t}^{\mathrm{in}} - f_{j,i,t}^{\mathrm{out}}, \quad \forall (i,j) \in A, t > 1, \tag{14}$$

$$L_{i,j,t} \ge L_{i,j}^0, \quad \forall (i,j) \in A, t = 24, \tag{15}$$

Minimum and maximum limits for pressure, gas flow in pipes and gas supply from terminals were imposed by inequalities (2)-(4). Constraint (5) ensures the mass balance at each node i in each time step. Gas flow inside a pipe was assumed to be in steady state and the Weymouth equation (6) was used, the coefficient, $K_{i,j}$ is related to the pipe parameters (pipe size, friction factor, etc) which can be calculated by $K_{i,j} = \frac{2.049R^{5.33}}{ZrLT_b}$. Variables $f^+_{i,j,t}$, was used to express the average value of positive flow (7) while$f^-_{i,j,t}$ was used to express the average value of negative flow (8) in a pipe. A set of binary variables $x_{i,j,t}$ and a sufficiently large positive value M were used to determine the direction of gas flow in pipes, and ensure only one of constraints (9) and (10) is active. Then, the bidirectional flow can be expressed by (11). Note that if $x_{i,j,t} = 1$, $f_{i,j,t} = f^+_{i,j,t}$, $p_{i,t} - p_{j,t} \geq 0$, the direction of gas flow is positive (from i to j), on the contrary, if $x_{i,j,t} = 0$, $f_{i,j,t} = -f^-_{i,j,t}$, $p_{i,t} - p_{j,t} \leq 0$, the direction of gas flow is negative (from j to i). (12) expresses the relationship between the volume of linepack in a pipe and the pressure at both ends of this pipe, $S_{i,j}$ is the coefficient related to the pipe parameters which can be calculated by $S_{i,j} = \frac{\pi LR^2}{4ZrT_b}$. (13) and (14) indicate the fluctuation of linepack during each time step, where (13) gives the relationship between linepack value of the first step and the value of the initial linepack. To ensure the level of linepack is sufficient for the next day, linepack at $t = 24$ is required to equal or greater than the initial volume of linepack as (15) expresses.

B. MISOCP FORMULATION AND BOUND-TIGHTENING ALGORITHM

Because constraint (6) makes the problem nonlinear and nonconvex, MISOCP was employed to approximate it for reducing computational complexity.

(16)-(19) convert the nonlinear gas flow equation (6) to a SOC formulation. Firstly, (6) was replaced by a pair of constraints (16) and (17), remaining (16) only and adding an auxiliary variable $\varphi_{i,j,t} = p^2_{j,t} - p^2_{i,t}$, then relaxing (16) by replacing it with (18) and (19).

$$f_{i,j,t}\left|f_{i,j,t}\right| \leq K^2_{i,j}\left(p^2_{i,t} - p^2_{j,t}\right), \quad \forall (i,j) \in A, t, \tag{16}$$

$$f_{i,j,t}\left|f_{i,j,t}\right| \geq K^2_{i,j}\left(p^2_{i,t} - p^2_{j,t}\right), \quad \forall (i,j) \in A, t, \tag{17}$$

$$(f^+_{i,j,t})^2 \leq K^2_{i,j}\varphi_{i,j,t} + M^2(1 - x_{i,j,t}), \quad \forall (i,j) \in A, t, \tag{18}$$

$$(f^-_{i,j,t})^2 \leq -K^2_{i,j}\varphi_{i,j,t} + M^2 x_{i,j,t}, \quad \forall (i,j) \in A, t, \tag{19}$$

The MISOCP problem was formulated with a McCormick envelope which can be found in (40)-(43) in Appendix A. However, as there is a trade-off between the accuracy of the solution and the computational time: over-relaxed bounds of SOC constraints give fast calculation but may produce inaccurate solutions while over-tightening bounds of them results in increased time though increased accuracy. Fig.1 graphically shows the impact of SOC bounds on model accuracy. To address this, a bound-tightening algorithm proposed by [8] was employed. The detail of the algorithm is explained in Appendix B.

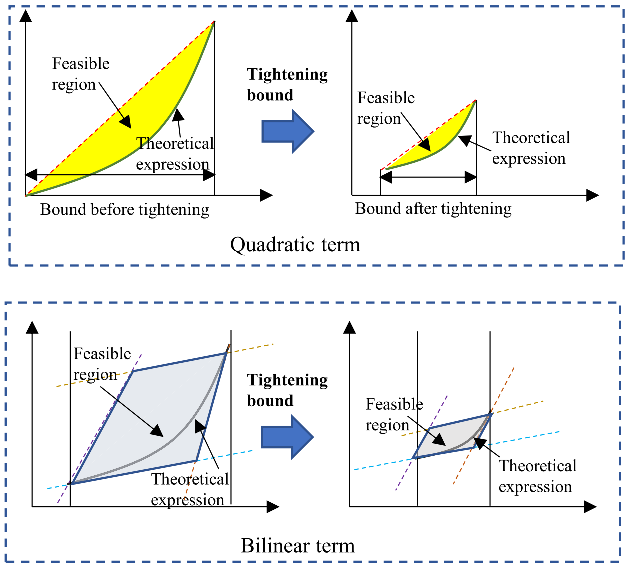

FIGURE 1. Tightening the bound of the SOC constraints.

C. MODELLING OF THE COMPRESSOR UNITS

Compressor units installed in a gas transmission network boost the pressure to ensure gas can be delivered from supply sites to end users. Within each compressor station there could be several compressor units that can be configured in series or parallel to achieve the required pressure boost and gas throughput. A compressor unit has to work within an operating envelope enclosed by four curves as shown in Fig. 2(a). This indicates the relationship between the compression ratio and flow rate at various operating speed of a compressor which can be expressed by a group of inequities (20), where f_k is the nonlinear function. To reduce computational complexity, these four curves are simplified to straight lines as shown in Fig. 2 (b), which can be expressed by (21) [7], where f'_k is the linear function.

$$f_k\left(Q_c, \alpha\right) \leq 0, \quad k = 1, 2, 3, 4 \tag{20}$$

$$f'_k\left(Q_c, \alpha\right) = \theta_k Q_c + \theta'_k \alpha + \theta''_k \leq 0, \quad k = 1, 2, 3, 4 \tag{21}$$

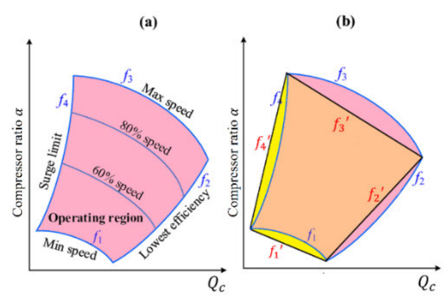

FIGURE 2. Theoretical envelope (a) and approximated envelope (b) of a compressor [7].

In the case study, two types of compressor units operating in parallel were modelled as shown in Fig. 3. There are three valves that are used to control the direction of gas flow. If the compressor units are in the OFF state, the valve 1 allows gas flow though the bypass line only. If the compressor station operates to boost the pressure, gas flow will be directed to either of the compressor units (GDC or EDC) under the control of valve 2 and valve 3. The pressure increase of gas flow was expressed by (22). Where the p_i is the pressure at suction node and $p_j$is the pressure at discharge node, and this bilinear term was relaxed by using McCormick relaxation which can be found in (48)-(51) in Appendix A.

$$p_{j,t} = \alpha_{i,j,t} p_{i,t}, \quad \forall (i,j) \in C, t \tag{22}$$

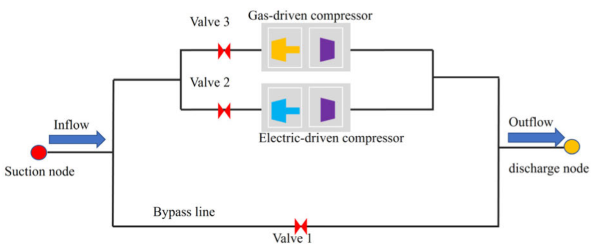

FIGURE 3. Parallel configuration of compressor units.

The energy consumption of a compressor is a function of the volume of gas throughput and the compression ratio (23):

$$P_{c,t} = \frac{m}{\eta(m-1)} Q_{c,t} \left(\alpha_{c,t}^{\frac{m-1}{m}} - 1 \right), \quad \forall c, t \tag{23}$$

The gas consumed by the GDC was calculated as (24), and the mass balance at the suction node of the GDC was expressed by (25). There is no negative flow through any compressor because gas can only flow from the suction node to discharge node, as (26) and (27) expresses:

$$Q'_{g,t} = \frac{P_{g,t}}{\emptyset}, \quad \forall g, t \tag{24}$$

$$Q_{c,t} + Q'_{g,t} = f_{i,j,t}^{\text{in}}, \quad \forall c \in G, \ \forall g, \ \forall (i,j) \in G, t \tag{25}$$

$$f_{j,i,t}^{\text{in}} = 0, \quad \forall (i,j) \in C, t \tag{26}$$

$$f_{j,i,t}^{\text{out}} = 0, \quad \forall (i,j) \in C, t \tag{27}$$

The nonlinear expression (23) was simplified to a linear equation (28) by fitting the data from it. Then, two sets of binary variables $y_{c,t}$, $y'_{c,t}$ were introduced to control different operating modes of a compressor. Operation states of a compressor unit were expressed by (29)-(32).

$$P_{c,t} = BQ_{c,t} + B'\alpha_{c,t}, \quad \forall c, t \tag{28}$$

$$P_{c,t} \geq BQ_{c,t} + B'\alpha_{c,t} - M_2 \left(1 - y_{c,t}\right), \quad \forall c, t \tag{29}$$

$$P_{c,t} \leq BQ_{c,t} + B'\alpha_{c,t} + M_2 \left(1 - y_{c,t}\right), \quad \forall c, t \tag{30}$$

$$0 \leq P_{c,t} \leq M_2 y_{c,t}, \quad \forall c, t \tag{31}$$

$$M_4 y_{c,t} \leq \alpha_{c,t} - 1 \leq M_3 y_{c,t}, \quad \forall c, t \tag{32}$$

where M_2 and M_3 are two big values and M_4 is a sufficiently small value. These constants with $y_{c,t}$ are used to ensure only if the compressor ratio is larger than 1, the energy will be consumed to drive the compressor to boost to pressure: when $y_{c,t} = 1$, $P_{c,t} = BQ_{c,t} + B'\alpha_{c,t}$ and $\alpha_{c,t} > 1$ which indicates the compressor is working; when $y_{c,t} = 0$, $P_{c,t} = 0$ and $\alpha_{c,t} = 1$, the compressor is not working. If the compressor is working, then the option for operating GDC or EDC was expressed by (33)-(35).

$$0 \leq P_{g,t} \leq M_2 y'_{c,t} \tag{33}$$

$$0 \leq P_{e,t} \leq M_2 (1 - y'_{c,t}) \tag{34}$$

$$P_{c,t} = P_{g,t} + P_{e,t} \tag{35}$$

III. CASE STUDY

The high-pressure gas transmission system of South Wales and Southwest of England in UK was considered as a case study. To reduce the computational complexity, the transmission system was simplified to a network with 9 nodes, 7 pipelines and 2 compressor stations (indexed by a2 and a6). The topology of the gas network is shown as in Fig. 4. Each compressor station has two compressor units: one is electric-driven, and the other is gas-driven. The maximum capacity of each compressor unit is 35MW.

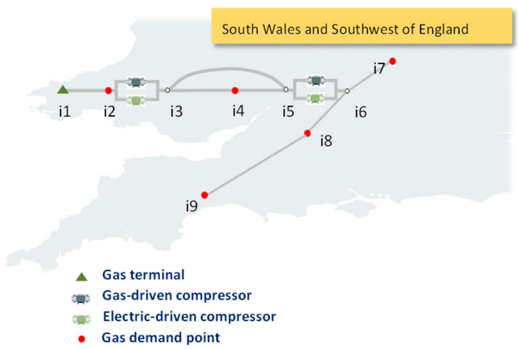

FIGURE 4. The gas network of South Wales and Southwest of England.

The profile of the hourly gas demand of a typical winter day, and the day-ahead prices of both gas and electricity are shown in Fig. 5. Pressure at gas terminal was fixed to 55 bar during 24 hours. The gas price was assumed to be constant during the day while the electricity price is fluctuating (the variation in electricity price was slightly exaggerated to test its impacts on the optimal operation of the compressors).

Three cases were studied in this paper:

- Case 1: Only GDCs are allowed to work
- Case 2: Only EDCs are allowed to work
- Case 3: Coordinated operation of GDCs and EDCs.

The MISOCP model was solved by Gurobi Optimizer 9.1.2 on the Python platform. A PC with Intel(R) Core (TM) i7-6700HQ 2.60GHz dual-core CPU was used.

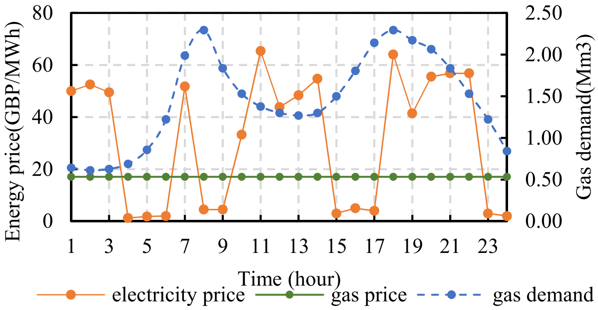

FIGURE 5. Hourly gas demand and day-ahead energy prices.

TABLE 1. Parameters and results of each iteration.

Iteration	γ_k	u^{av}	Iteration	Time
k=1	-	14.54%	k=1	3s
k=2	0.2	3.1%	k=2	18s
k=3	0.15	2.7%	k=3	31s

A. PERFORMANCE OF THE SOLUTION ALGORITHM

The accuracy of the model using bound-tightening algorithm was analysed. The number of iterations k was set to three (the algorithm was not used when $k = 1$). $e_{i,j,t}$ is the error between the value of gas flow in theoretical and that of the solution. $e_{i,j}^{av}$ in (36) is the average value of $e_{i,j,t}$ over time steps which was used to indicate the quality of the solution.

$$e_{i,j}^{av} = \frac{\sum_{t=1}^{T} e_{i,j,t}}{T}, \quad \forall (i,j) \in A \tag{36}$$

Fig. 6 shows the $e_{i,j}^{av}$ of each pipe after each iteration. Introducing $u^{av} = \frac{e_{i,j}^{av}}{N_A}$ to formulate the average value of the defined error $e_{i,j}^{av}$ of each pipeline, where N_A is the number of pipelines. Table 1 summarizes control parameters γ_k and results for each iteration. It can be found that the better solution with smaller u^{av} was obtained via tightening bound by the algorithm.

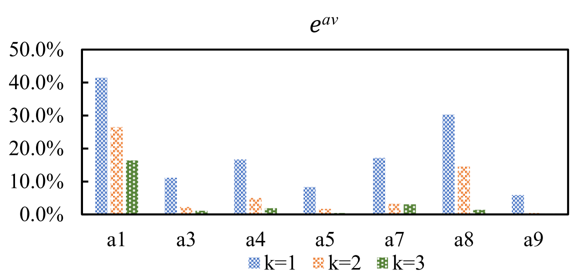

FIGURE 6. Improving solutions via using the bound-tightening algorithm.

The expressions of compression ratio were not included in SOC constraints, and their bounds are set relatively tightly, therefore, they are not enhanced by the bound-tightening algorithm. To validate the energy consumption of the compressor, the difference between the theoretical energy consumption and the optimised energy consumption of each compressor unit (case 3 based) was shown in Fig. 7.

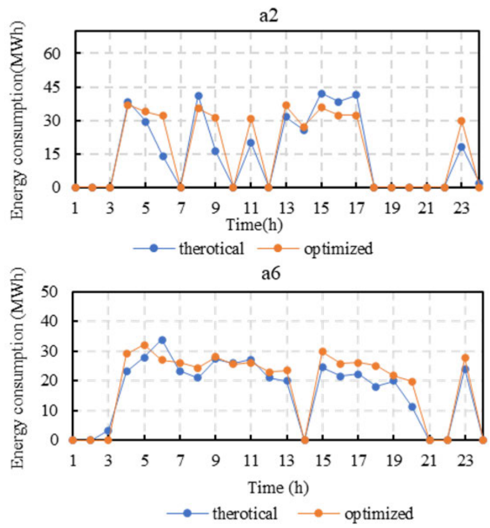

FIGURE 7. Validation of energy consumption of compressor units.

B. THE VALUE OF COORDINATED OPERATION OF GDC AND EDC

Three cases were investigated to determine the value of the combined operation of EDC and GDC. Profiles of the energy consumption in these cases were shown in Fig. 8, Fig. 9 and Fig. 10. Fig. 11 compares the hourly linepack of each case.

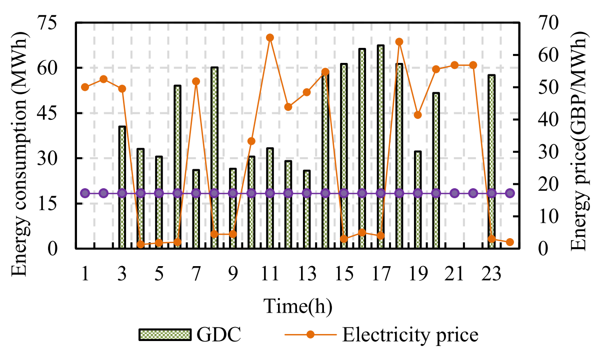

FIGURE 8. Energy consumption of compressors in case 1.

It can be found from Fig. 8, when only GDCs are allowed to work, the compressor works harder in period of higher gas demand (e.g., at hour 8, 17 and 18). However, when only EDCs are available, their operation is affected by the electricity price as shown in Fig.9. When electricity price is relatively lower (e.g., at hour 4, 5 and 6), compressor units will work harder to increase linepack. When electricity price is higher, the linepack can maintain the pressure for several hours and less energy was consumed by the compressor units.

Fig. 10 shows that the operation of GDCs and EDCs in Case 3 is sensitive to the relative price of electricity and gas: when the electricity cost is lower than that of gas (e.g., at hour 4, 5 and 6), EDCs are working (GDCs are OFF) and when

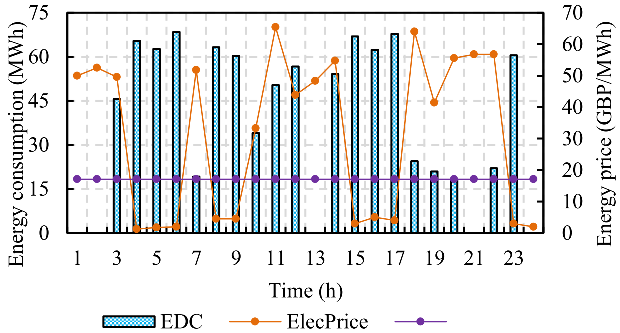

FIGURE 9. Energy consumption of compressors in case 2.

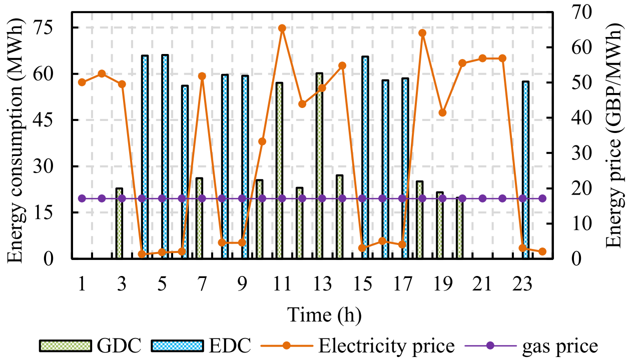

FIGURE 10. Energy consumption of compressors in case 3.

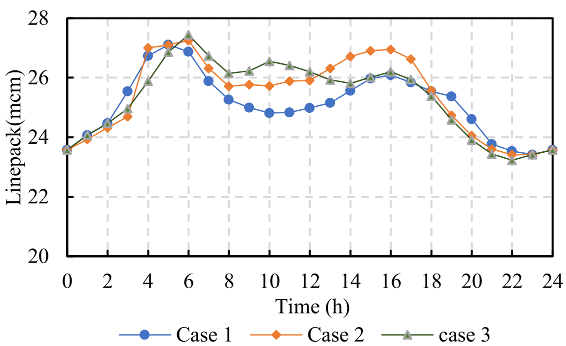

FIGURE 11. Linepack of the gas network in all cases.

the gas cost is lower (e.g., at hour 11, 13, 15), GDC is working (EDCs are OFF). In all three cases, in hour 23, the compressors work close to their rated capacity to ensure the 'end-of-day' target for linepack was met. Different operation strategies for the compressor units result in different linepack pattern as Fig.11 shown. Generally, the linepack of case 2 and case 3 are higher than that of case 1 because EDCs shift their operation in time to use low price electricity and therefore pressurise the network.

The operating costs for each case and emission of carbon dioxide from each operation schedule are listed below in Table 2 (1 m^3 natural gas produces 1.86 kg CO_2 [25]). It can be found that using EDC only produces no direct emission though, the cost of it is the highest among three cases.

TABLE 2. Cost of energy consumption and total emissions in all cases.

Case	EDC COST (GBP)	GDC cost (GBP)	Total cost (GBP)	CO_2 Emissions (tone/day)
Case 1	0	14461	14461	145.4
Case 2	19694	0	19694	0
Case 3	1741	5264	7006	52.9

The operating cost of the system in Case 3 is the lowest due to the coordinated operation of EDCs and GDCs allows exploiting low energy price for operating the compressors. Case 3 also produces only 36% of the carbon dioxide emissions of Case 1.

IV. CONCLUSION

The operation of a gas network with a combination of gas-driven and electric-driven compressor units was modelled to quantify the value of flexibility from compressor units. The mixed integer nonlinear optimisation problem was formulated as MISOCP. The problem was solved using an iterative bound-tightening algorithm to balance computational complexity and accuracy of the solution.

It was found that the algorithm is helpful for increasing accuracy of the model (decreased average value of defined error from 14.5% to 2.7%) while not dramatically increasing the computation time.

The coordinated operation of GDC and EDC is sensitive to the relative price of electricity to gas. Compared with only using GDC or EDC to boost the pressure, coordinated operation of GDC and EDC can save cost whilst producing lower emissions compared with using GDC only.

APPENDIX

A. RELAXATION OF SOC CONSTRAINTS

Constraints (18) and (19) are SOC formulations though, the auxiliary variable $\varphi_{i,j,t}$ was still expressed by the quadratic term $p_{i,t}^2 - p_{j,t}^2$. To address this, McCormick relaxation was employed to approximate it. Firstly, introducing two auxiliary variables $\pi_{i,j,t}^{+} = p_{i,t} + p_{j,t}$, $\pi_{i,j,t}^{-} = p_{i,t} - p_{j,t}$ that were constrained by (37) and (38). The quadratic term $p_{i,t}^2 - p_{j,t}^2$ was converted to a bilinear term as (39).

$$\underline{\pi}_{i,j,t}^{+} \leq \pi_{i,j,t}^{+} \leq \bar{\pi}_{i,j,t}^{+}, \quad \forall (i,j) \in A, t, \tag{37}$$

$$\underline{\pi}_{i,j,t}^{-} \leq \pi_{i,j,t}^{-} \leq \bar{\pi}_{i,j,t}^{-}, \quad \forall (i,j) \in A, t, \tag{38}$$

$$p_{i,t}^2 - p_{j,t}^2 = \pi_{i,j,t}^{+}\pi_{i,j,t}^{-}, \quad \forall (i,j) \in A, t, \tag{39}$$

Then, $\varphi_{i,j,t} = \pi_{i,j,t}^{+}\pi_{i,j,t}^{-}$ was relaxed by four linear expressions as (40)-(43):

$$\varphi_{i,j,t} \geq \bar{\pi}_{i,j,t}^{+}\pi_{i,j,t}^{-} + \pi_{i,j,t}^{+}\bar{\pi}_{i,j,t}^{-} - \bar{\pi}_{i,j,t}^{+}\bar{\pi}_{i,j,t}^{-} \tag{40}$$

$$\varphi_{i,j,t} \geq \underline{\pi}_{i,j,t}^{+}\pi_{i,j,t}^{-} + \pi_{i,j,t}^{+}\underline{\pi}_{i,j,t}^{-} - \underline{\pi}_{i,j,t}^{+}\underline{\pi}_{i,j,t}^{-} \tag{41}$$

$$\varphi_{i,j,t} \leq \bar{\pi}_{i,j,t}^{+}\pi_{i,j,t}^{-} + \pi_{i,j,t}^{+}\underline{\pi}_{i,j,t}^{-} - \bar{\pi}_{i,j,t}^{+}\underline{\pi}_{i,j,t}^{-} \tag{42}$$

$$\varphi_{i,j,t} \leq \underline{\pi}_{i,j,t}^{+}\pi_{i,j,t}^{-} + \pi_{i,j,t}^{+}\bar{\pi}_{i,j,t}^{-} - \underline{\pi}_{i,j,t}^{+}\bar{\pi}_{i,j,t}^{-} \tag{43}$$

Using additional auxiliary variables $w^{+}_{i,j,t}, w^{-}_{i,j,t}$ to convexly approximate $(f^{+}_{i,j,t})^2$ and $(f^{-}_{i,j,t})^2$ as expressed by (44)-(47).

$$w^{+}_{i,j,t} \geq (f^{+}_{i,j,t})^2 \tag{44}$$

$$w^{+}_{i,j,t} \leq \left(\bar{f}^{+}_{i,j,t} + \underline{f}^{+}_{i,j,t}\right) f^{+}_{i,j,t} - \bar{f}^{+}_{i,j,t}\underline{f}^{+}_{i,j,t} \tag{45}$$

$$w^{-}_{i,j,t} \geq (f^{-}_{i,j,t})^2 \tag{46}$$

$$w^{-}_{i,j,t} \leq (\bar{f}^{-}_{i,j,t} + \underline{f}^{-}_{i,j,t}) f^{-}_{i,j,t} - \bar{f}^{-}_{i,j,t}\underline{f}^{-}_{i,j,t} \tag{47}$$

More, McCormick relaxation was used to approximate the expression of compressing ratio (22) through an envelope bounded by (48)-(51):

$$p_{j,t} \leq \alpha^{\max}_{i,j} p_{i,t} + \alpha_{i,j} p^{\min}_{i,t} - p^{\min}_{i,t}\alpha^{\max}_{i,j} \tag{48}$$

$$p_{j,t} \leq \alpha^{\min}_{i,j} p_{i,t} + \alpha_{i,j,t} p^{\max}_{i,t} - p^{\max}_{i,t}\alpha^{\min}_{i,j} \tag{49}$$

$$p_{j,t} \geq \alpha^{\max}_{i,j} p_{i,t} + \alpha_{i,j,t} p^{\max}_{i,t} - p^{\max}_{i,t}\alpha^{\max}_{i,j} \tag{50}$$

$$p_{j,t} \geq \alpha^{\min}_{i,j} p_{i,t} + \alpha_{i,j,t} p^{\min}_{i,t} - p^{\min}_{i,t}\alpha^{\min}_{i,j} \tag{51}$$

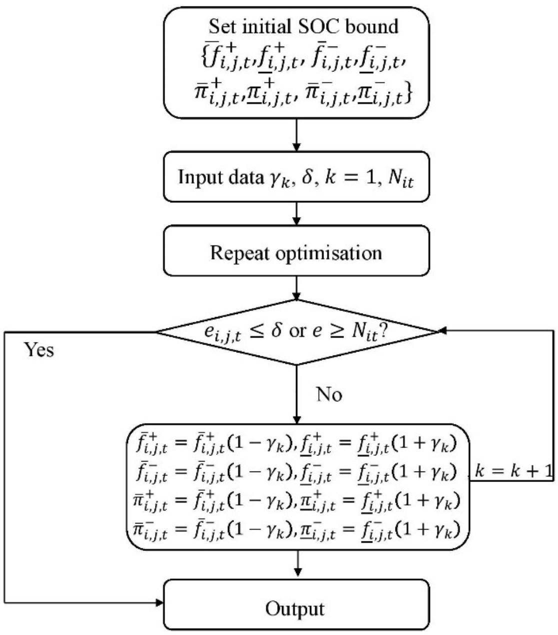

FIGURE 12. **Function of the algorithm.**

B. BOUND-TIGHTENING APPROACH

The function of the bound-tightening algorithm was clarified in this section as shown in Fig. 12. A set of control parameters γ_k (unique for each pipeline at each iteration) which were used to increase the value of the lower bound or decrease the value of the upper bound, were introduced firstly. Initially, the bounds of each SOC constraint $\{\bar{f}^{+}_{i,j,t}, \underline{f}^{+}_{i,j,t}, \bar{f}^{-}_{i,j,t}, \underline{f}^{-}_{i,j,t}, \bar{\pi}^{+}_{i,j,t}$[[space]], $\underline{\pi}^{+}_{i,j,t}, \bar{\pi}^{-}_{i,j,t}$[[space]], $\underline{\pi}^{-}_{i,j,t}\}$ were created in relatively wide ranges. Then the optimization will be solved repeatedly until the defined error is less than the set convergence tolerance δ or a number of iterations (N_{it}) were completed. The error used to control the repetition was defined as in (52) [8].

$$e_{i,j,t} = \frac{K^2_{i,j}(p^2_{i,t} - p^2_{j,t}) - f^2_{i,j}}{K^2_{i,j}(p^2_{i,t} - p^2_{j,t})} \times 100\% \tag{52}$$

REFERENCES

[1] National Grid. (2020). *Gas Ten Year Statement 2020*. [Online]. Available: https://www.nationalgrid.com/uk/gas-transmission/insight-and-innovation/gas-ten-year-statement-gtys
[2] S. Clegg and P. Mancarella, "Integrated electrical and gas network flexibility assessment in low-carbon multi-energy systems," *IEEE Trans. Sustain. Energy*, vol. 7, no. 2, pp. 718–731, Apr. 2016.
[3] H. Ameli, M. Qadrdan, and G. Strbac, "Value of gas network infrastructure flexibility in supporting cost effective operation of power systems," *Appl. Energy*, vol. 202, pp. 571–580, Sep. 2017.
[4] S. Clegg and P. Mancarella, "Storing renewables in the gas network: Modelling of power-to-gas seasonal storage flexibility in low-carbon power systems," *IET Gener., Transmiss. Distribution*, vol. 10, no. 3, pp. 566–575, Feb. 2016.
[5] C. O'Malley, S. Delikaraoglou, L. Roald, and G. Hug, "Natural gas system dispatch accounting for electricity side flexibility," *Electric Power Syst. Res.*, vol. 178, Jan. 2020, Art. no. 106038.
[6] OFGEM. (Jun. 2019). *Compressor Emissions Compliance Strategy Guidance*. [Online]. Available: https://www.ofgem.gov.uk/sites/default/files/docs/2019/06/compressor_emissions_compliance_guidance.pdf
[7] Y. Zhao, X. Xu, M. Qadrdan, and J. Wu, "Optimal operation of compressor units in gas networks to provide flexibility to power systems," *Appl. Energy*, vol. 290, May 2021, Art. no. 116740.
[8] S. Chen, A. J. Conejo, R. Sioshansi, and Z. Wei, "Unit commitment with an enhanced natural gas-flow model," *IEEE Trans. Power Syst.*, vol. 34, no. 5, pp. 3729–3738, Sep. 2019.
[9] A. Schwele, A. Arrigo, C. Vervaeren, J. Kazempour, and F. Vallée, "Coordination of electricity, heat, and natural gas systems accounting for network flexibility," *Electric Power Syst. Res.*, vol. 189, Dec. 2020, Art. no. 106776.
[10] A. Ratha, A. Schwele, J. Kazempour, P. Pinson, S. S. Torbaghan, and A. Virag, "Affine policies for flexibility provision by natural gas networks to power systems," *Electric Power Syst. Res.*, vol. 189, Dec. 2020, Art. no. 106565.
[11] R. L. Meira, G. M. N. Costa, R. A. Kalid, and M. A. F. Martins, "Improving the centrifugal compressor map through rigorous thermodynamic modeling: An analysis on a natural gas compression station pipeline," *J. Natural Gas Sci. Eng.*, vol. 92, Aug. 2021, Art. no. 104006.
[12] M. S. Delshad, A. Momenimovahed, M. S. Mazidi, M. A. Ehyaei, and M. A. Rosen, "Energy, exergy, exergoenvironmental, and exergoeconomic (4E) analyses of a gas boosting station," *Energy Sci. Eng.*, vol. 9, no. 11, pp. 2044–2063, Nov. 2021.
[13] P. Milosavljevic, A. G. Marchetti, A. Cortinovis, T. Faulwasser, M. Mercangöz, and D. Bonvin, "Real-time optimization of load sharing for gas compressors in the presence of uncertainty," *Appl. Energy*, vol. 272, Aug. 2020, Art. no. 114883.
[14] Y. Wang, Y. Wang, Y. Huang, J. Yang, Y. Ma, H. Yu, M. Zeng, F. Zhang, and Y. Zhang, "Operation optimization of regional integrated energy system based on the modeling of electricity-thermal-natural gas network," *Appl. Energy*, vol. 251, Oct. 2019, Art. no. 113410.
[15] Y. Jiang, J. Xu, Y. Sun, C. Wei, J. Wang, S. Liao, D. Ke, X. Li, J. Yang, and X. Peng, "Coordinated operation of gas-electricity integrated distribution system with multi-CCHP and distributed renewable energy sources," *Appl. Energy*, vol. 211, pp. 237–248, Feb. 2018.
[16] Q. Zeng, B. Zhang, J. Fang, and Z. Chen, "A Bi-level programming for multistage co-expansion planning of the integrated gas and electricity system," *Appl. Energy*, vol. 200, pp. 192–203, Aug. 2017.
[17] V. Khaligh, M. O. Buygi, A. Anvari-Moghaddam, and J. M. Guerrero, "A multi-attribute expansion planning model for integrated gas–electricity system," *Energies*, vol. 11, no. 10, p. 2573, Sep. 2018.
[18] G. Sun, S. Chen, Z. Wei, and S. Chen, "Multi-period integrated natural gas and electric power system probabilistic optimal power flow incorporating power-to-gas units," *J. Mod. Power Syst. Clean Energy*, vol. 5, no. 3, pp. 412–423, 2017.

[19] J. Yang, N. Zhang, A. Botterud, and C. Kang, "Situation awareness of electricity-gas coupled systems with a multi-port equivalent gas network model," *Appl. Energy*, vol. 258, Jan. 2020, Art. no. 114029.
[20] Y.-Q. Bao, M. Wu, X. Zhou, and X. Tang, "Piecewise linear approximation of gas flow function for the optimization of integrated electricity and natural gas system," *IEEE Access*, vol. 7, pp. 91819–91826, 2019.
[21] L. Yao, X. Wang, T. Ding, Y. Wang, X. Wu, and J. Liu, "Stochastic day-ahead scheduling of integrated energy distribution network with identifying redundant gas network constraints," *IEEE Trans. Smart Grid*, vol. 10, no. 4, pp. 4309–4322, Jul. 2019.
[22] C. Wang, W. Wei, J. Wang, L. Wu, and Y. Liang, "Equilibrium of interdependent gas and electricity markets with marginal price based bilateral energy trading," *IEEE Trans. Power Syst.*, vol. 33, no. 5, pp. 4854–4867, Sep. 2018.
[23] H. Yang, P. You, and C. Shang, "Distributed planning of electricity and natural gas networks and energy hubs," *Appl. Energy*, vol. 282, Jan. 2021, Art. no. 116090.
[24] A. Schwele, C. Ordoudis, J. Kazempour, and P. Pinson, "Coordination of power and natural gas systems: Convexification approaches for linepack modeling," in *Proc. IEEE Milan PowerTech*, Jun. 2019, pp. 1–6.
[25] D. Willms and L. Brubacher, "What is your carbon footprint? Chem 13 news," Univ. Waterloo, Waterloo, ON, Canada, Tech. Rep., Nov. 2007.

QIKUN CHEN is currently pursuing the Ph.D. degree with the Centre for Integrated Renewable Energy Generation and Supply (CIREGS), Cardiff University. His research interests include the flexibility of the integrated energy systems, modeling, and optimization.

YONGNING ZHAO received the B.Sc. and Ph.D. degrees in electrical engineering from China Agricultural University (CAU), Beijing, China, in 2012 and 2018, respectively. He was a Research Associate at Cardiff University, from 2019 to 2021. He is currently an Associate Professor at CAU. His research interests include renewable energy integration, optimization, and power/energy system dispatch.

MEYSAM QADRDAN (Senior Member, IEEE) is with the School of Engineering, Cardiff University. His research interests include modeling and analysis of short-term operation and long-term expansion of integrated energy systems.

NICHOLAS JENKINS (Fellow, IEEE) received the B.Sc. degree from Southampton University, Southampton, U.K., in 1974, the M.Sc. degree from Reading University, Reading, U.K., in 1975, and the Ph.D. degree from the Imperial College London, London, U.K., in 1986. He is currently a Professor with Cardiff University, Cardiff, U.K. Before moving to academia, his career included 14 years of industrial experience of which five years were in developing countries. While at university, he has developed teaching and research activities in both electrical power engineering and renewable energy.